Journal of Power Sources Advances 42 (2026) 100218

Contents lists available at ScienceDirect

Journal of Power Sources Advances

journal homepage: www.sciencedirect.com/journal/journal-of-power-sources-advances

Potential of a Honda fuel cell module developed for mobility applications in stationary CHP configuration

Antonius Tilgner [a,*], Johannes Seesing [a], Heinz Bekebrok [a], Marco Ohm [a], Alexander Dyck [a], Sebastian Barth [b], Florian Rass [b], Yannick Arz [b], Thomas Brachmann [b], Hendrik Langnickel [a]

[a] German Aerospace Center, Institute of Networked Energy Systems, Oldenburg, Germany
[b] Honda R&D Europe (Deutschland) GmbH, Offenbach, Germany

ARTICLE INFO

Keywords:
Hydrogen fuel cell CHP
Stationary application
Efficiency
Characteristics
PEM fuel cell

ABSTRACT

This study presents for the first time the results of a test bench evaluation of a 78 kW_{el} Honda fuel cell module, originally designed for mobile applications, in a stationary combined heat and power (CHP) configuration. The module's performance was assessed at various return temperatures (40, 50, and, 60 °C) and power setpoints. Notably, the results show very efficient operation across the temperatures and power setpoints. The module achieved thermal and electrical efficiencies of over 54% and 50%, respectively, with a total efficiency of up to 97.1% with respect to the high heating value (HHV) of hydrogen. Furthermore, the hydrogen content in the exhaust gas was analyzed and the results show almost no hydrogen in the stream. These findings suggest that the Honda fuel cell module has significant potential as a highly efficient stationary power source, offering improved performance compared to commercially available hydrogen engine CHP systems, e.g. hydrogen internal combustion engines.

1. Introduction

In a future decarbonized energy system, hydrogen electrolyzed from renewable energies and its derivatives are key components as an energy carrier and raw material for the chemical industry [1]. Together with its capacity as a flexibility to mitigate grid imbalances, these are highly useful and necessary qualities for such a future energy system [2].

In theory, direct use of electrical energy is always preferable to conversion and storage due to the additional infrastructure necessary and the energy losses from conversion and storage. Therefore, when reconverting hydrogen into electricity, technical solutions with high efficiency should be used. In addition to increasing efficiency, coupling energy sectors such as consumers, producers, converters, storage facilities and necessary infrastructure can offer flexibility and resilience for the energy system [3]. Decentralized approaches enable the required spatial proximity for successful sector coupling, such as the energetic connection of residential and commercial areas. Furthermore, decentralized approaches also show potential in reducing distribution losses and conversion losses, further increasing efficiency [4].

Fuel Cells (FC) generating electricity from hydrogen while recovering the generated waste heat as part of a Combined Heat and Power (CHP) system provide high efficiency and potential for stationary, decentralized operation [5]. Most studies investigating residential FC CHP systems are covering micro-CHP systems in a power range of 0.5–5 kW [6]. Micro-CHP systems play a large role in Japan, where more than 400,000 units have been installed in households since 2009 within the scope of the ENE-FARM project [5]. Although these systems do experience economic success, the initial capital costs remain high [7]. While the micro-CHP power range has been thoroughly investigated reaching efficiencies of up to 92% [6,8–12], systems in higher power ranges have been analyzed much less. CHP systems in higher power classes supplying a larger number of recipients at once might result in a more economic operation due to increased capacity utilization [6]. A possibility of addressing the high initial capital costs can be economies of scale [6,13]. Technically mature FC modules that are thoroughly tested and optimized and that leverage economies of scale can be found in the automotive sector, where serial production infrastructure is already in place. Such modules are technically available from Honda [14]. These FC systems with 78 kW_{el} power output have a high electrical efficiency with respect to the high heating value (HHV) of > 50 % and a long lifetime in automotive applications. In stationary applications, the thermal power can be utilized in addition to the electrical power, greatly increasing the overall efficiency of the

* Corresponding author.
E-mail address: antonius.tilgner@dlr.de (A. Tilgner).

https://doi.org/10.1016/j.powera.2026.100218
Received 23 March 2026; Received in revised form 29 July 2026; Accepted 16 September 2026
Available online 8 October 2026
2666-2485/© 2026 The Authors. Published by Elsevier Ltd. This is an open access article under the CC BY license (http://creativecommons.org/licenses/by/4.0/).
Open access funding enabled and organized by Projekt DEAL.

Table 1
An overview of similar studies. Most available experimental studies offer limited comparability due to different scopes and/or investigated power classes.

Methodology	Scope	Power range (electric)	Key outcome	Comment on comparability
Experimental	Tailpipe emissions FCEV	N/A	H_2-emissions up to 14 vol.% [23]	Unknown power class; Whole vehicle on testbench; Different measurement techniques; Non-comparable load profile
Experimental	FCEV on testbench	130 kW	H_2-emissions >1 vol.%, 87-93% efficiency [17]	Whole vehicle on testbench; Different system boundaries and measurement techniques (e.g. electrical efficiency calculation focusses mainly on stack and not on system level)
Experimental	Multistack	180 kW	92% total efficiency [24]	Not system, but stack level investigation; Different powerclass
Experimental	PEMFC CHP with ORC	65 kW	75.5% total efficiency [25]	Different method of heat recovery
Experimental	PEMFC without heat recovery	130 kW	51% electrical efficiency [26]	No heat recovery; Stack level investigation
Experimental	PEMFC CHP	1-2 kW	89-92% total efficiency [9,27]	Different power class
Simulation	Simulations of different scopes	N/A	N/A	[28–32]

system and making it suitable for stationary residential application, where the simultaneous supply of heat and power is desired and necessary [8]. While it has been simulated that fuel cell powered electric vehicles (FCEVs) are able to provide heat and power to residential areas, a transition from mobility application to a complete stationary application has not yet been experimentally explored [15,16]. Comprehensive efficiency analyses of FCs in stationary CHP application and in comparable power classes are scarce, with existing studies limited to the electrical side and to stack-level investigations and often relying on simplified modeling and investigation rather than experimental validation [17–21]. An overview of selected studies can be seen in Table 1. In residential application, operation with reduced dynamics compared to mobile applications can be expected, increasing the FC module's lifetime and therefore its economic viability. Furthermore, these systems also offer options for auxiliary support in fast EV charging and local decentralized electrical grid stabilization [22].

This study explores the possibility of transferring mature FC modules designed for automotive application to a stationary CHP application without further adjustment of the module or its internal control mechanisms. After a short description of the test setup and the data basis, we present the results of the efficiency tests for the first stationary operation of this FC module in CHP configuration including hydrogen measurements in the exhaust flow.

2. Methodology

2.1. Description of the test setup

Operating the FC module on a stationary test bench requires various control mechanisms and an extensive hydraulic setup comprising valves, heat exchangers, pumps and sensors. A schematic and simplified flowchart with all essential elements, flows and sensors can be seen in Fig. 1. In Table A.2 the sensors including uncertainties and types are listed. All sensors have been calibrated with a standardized procedure before the tests and the measurements have been verified. The FC module, which is new and has not been operated before our tests, is supplied with hydrogen in quality 5.0 (> 99.999% purity) at 10 bar relative pressure and ambient air, which is compressed within the module before being fed into the stack. All tests are conducted in a controlled testing environment. Before being supplied to the stack, the air is heated and humidified [14].

Two cooling circuits dissipate the heat of the system to be recovered as part of the CHP application. In addition to the stack cooling, the Balance of Plant (BOP) cooling circuit dissipates the heat from the compressed ambient air, the air compressor itself and the power electronics within the module. An external heat exchanger is built into both circuits to recover the heat, which is subsequently fed into different sinks. All external pipes are insulated and the temperatures are measured directly within the pipes using the PT100 temperature sensors A.2. The return temperature of both circuits can be set and controlled. The control of the return temperature is carried out by controlling the temperature of the heat sinks of the respective cooling circuits.

2.2. Data basis

The data used for the evaluation is logged with a frequency of 1 Hz. Tests were executed in net electrical output power steps of 10 kW from 10 kW to 70 kW. This corresponds to the power measured after the power for the system operation (e.g. the air compressor) is fed back to the module. At each power level two measurements with an evaluation time span of 30 min were executed, in order to obtain a robust mean value and minimize errors. In a first measurement the power level was approached from a lower power level and in a second measurement from a higher power level, in order to account for potentially different behavior of the module in the two cases and obtain a robust and representative data basis. The methodology was kept although no difference in behavior was observed. In both cases the evaluation period only started when the system had fully stabilized. The steady-state was identified based on visual inspection of the live data. The data from the two evaluation periods are then merged to obtain 3600 data points for each power level. These measurements were conducted in three cycles, each for a different return temperature of the FC coolant circuit, specifically 40, 50, and, 60 °C.

2.3. Efficiency calculation

The system borders are defined at the external heat exchangers of the BOP and FC circuits for the outputs, as well as at the H_2 valve for the input. In Fig. 1 the system borders forming the basis for the efficiency calculation are depicted as a dashed line. The thermal power extracted from the BOP and FC cooling circuits is calculated between the respective sink and heat exchanger (Fig. 1) via

$$\dot{Q} = \dot{V} \cdot \rho_{water} \cdot c_{p,water} \cdot (T_2 - T_1). \quad (1)$$

Due to short distances to the module and strong insulation, this can be determined as a meaningful measuring point.

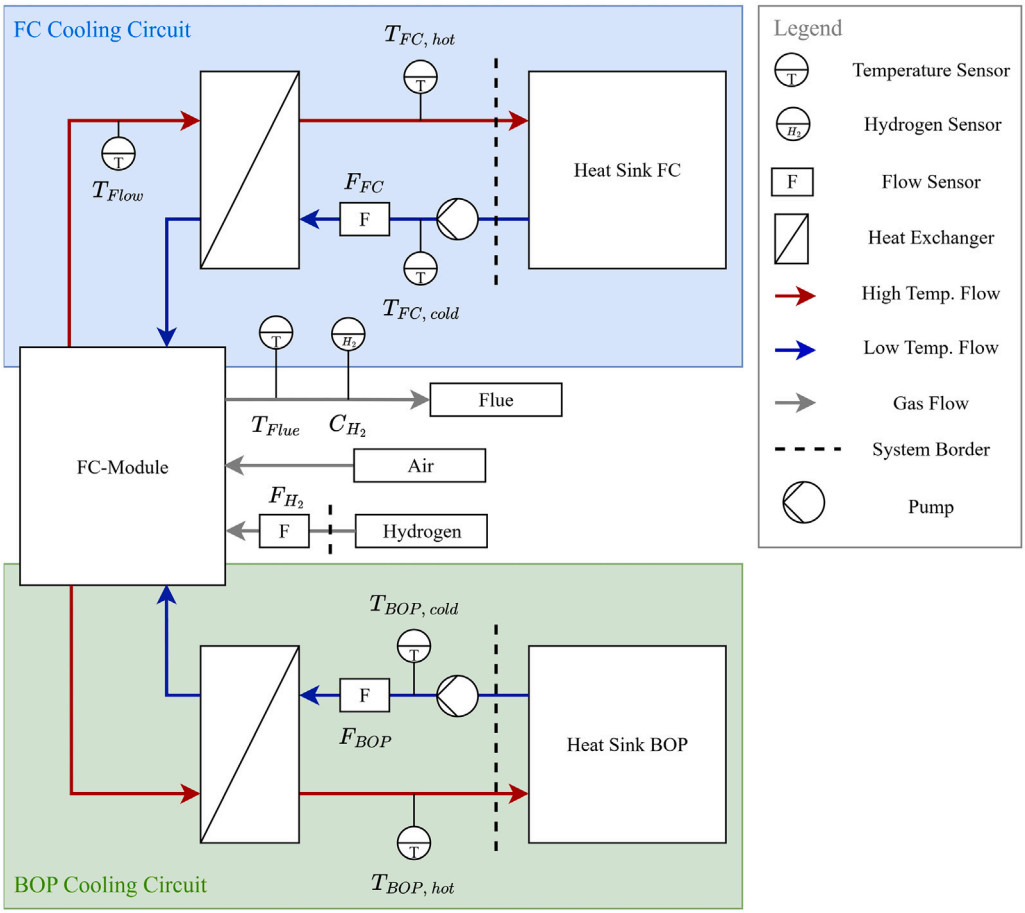


Fig. 1. Schematic flowchart of the hydraulic test bench setup. The flowchart is divided into two cooling circuits: the Balance of Plant (BOP) circuit dissipates the heat from auxiliary subsystems such as the air compressor while the FC cooling circuit dissipates the heat from the FC-stack. All relevant temperature and flow sensors for the calculation of the efficiency are depicted. The corresponding sensor types are presented in Table A.2. The colors of the arrows represent the relative fluid temperatures.

The input power at the H_2 valve is defined as the theoretical chemical power of the hydrogen fed into the module, while the output power is the sum of the electrical and thermal powers (2). It should be noted that for the efficiency calculation the HHV of hydrogen was used rather than the lower heating value (LHV). This is due to the efficiencies reaching above 100% when using the LHV to calculate the chemical energy in the hydrogen.

$$\bar{\eta}_{total} = \frac{\bar{P}_{out}}{\bar{P}_{in}} = \bar{\eta}_{therm} + \bar{\eta}_{el} \tag{2}$$

With the thermal efficiency being calculated via

$$\bar{\eta}_{therm} = \frac{\bar{Q}_{BOP} + \bar{Q}_{FC}}{\bar{P}_{chem}} \tag{3}$$

and the electrical efficiency via

$$\bar{\eta}_{el} = \frac{\bar{P}_{el}}{\bar{P}_{chem}}. \tag{4}$$

For the calculation of the efficiencies the mean values for the thermal powers (1) across the one-hour evaluation period are used.

3. Results and discussion

In this section, selected results obtained from the conducted analysis are presented. The markers represent the mean values calculated over a one-hour evaluation period at each power level. The errors of the sensors can be found in A.2, while the location of the sensors on the testbench is depicted in Fig. 1. In the two plots, that do not show directly measured, but rather calculated values (Fig. 4 and Fig. 5), the error bars show the calculated error according to error propagation theory [33]. To visualize the general trends and the differences between the test configurations, the values are connected by dashed lines. These lines are solely for visualization purposes and do not represent known values.

To assess the needed infrastructure for the stationary application of this module, the concentration of hydrogen in the exhaust gas is an important characteristic. In 2.1 it is depicted as a function of the electrical power setpoint. During the evaluation period we observed nearly no hydrogen ejected via the exhaust gas. Apart from two very short ejections (about 2 s) of hydrogen, we did not detect any hydrogen in the exhaust gas. These ejections have a very small magnitude close to the detection limit of the sensor (0.2 vol.%$_{H_2}$). The exact reason for these two events is unknown, but as they are both very short and just barely detectable, they are not further considered. As generally only

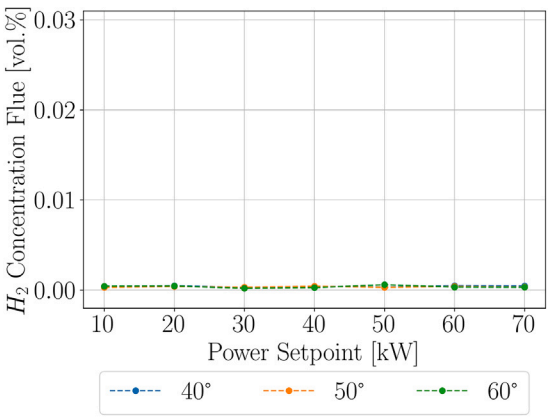


Fig. 2.1. H_2 Concentration in the exhaust. Very little hydrogen is ejected via the exhaust (C_{H_2}, see Fig. 1). The high standard deviation at 50 kW and 70 kW for 60 °C and 40 °C respectively is due to very short times, where up to 0.1 vol.% hydrogen were ejected in the corresponding evaluation period.

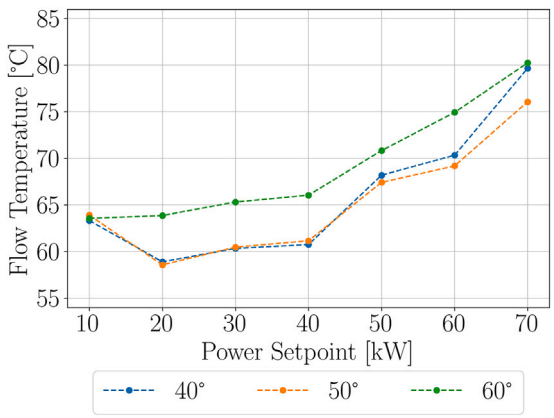


Fig. 3.1. FC Flow Temperature. The flow temperature of the FC circuit (T_{Flow}, see Fig. 1) generally rises with higher power setpoint. For 40 °C and 50 °C return temperature, the flow temperature is similar, while it becomes higher at 60 °C.

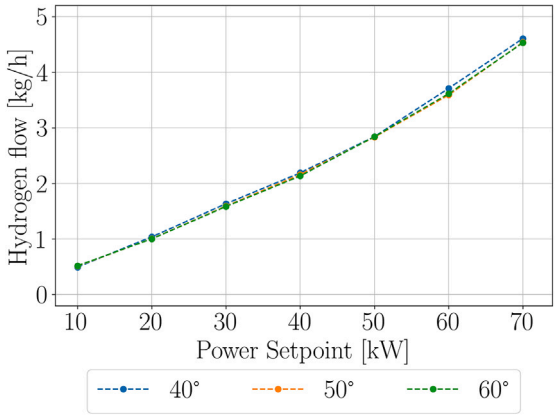


Fig. 2.2. Hydrogen Flow. The hydrogen consumption (F_{H_2}, see Fig. 1) does not change significantly with different FC return temperatures. For higher power setpoints, more hydrogen is supplied.

minuscule amounts of hydrogen are ejected, almost all hydrogen supplied is converted into electrical and thermal energy. This result marks a significant improvement compared to previous studies studying the exhaust emissions of FCEVs. Alves et al. (2025) [17] measured significant hydrogen emissions at the tailpipe of a FCEV on a testbench under steady driving conditions. Pearman et al. (2023) [23] also measured significant hydrogen emissions, but under variable standardized driving conditions. It should be noted that both studies operated the whole car on a testbench instead of only the FC module, which could impact the comparability of these results with our own. The absence of hydrogen in the exhaust is a benefit for residential application, as no further infrastructure (e.g. hydrogen afterburner) has to be implemented in order to prevent the formation of explosive atmospheres at the outlet of the exhaust gas.

The hydrogen demand in kg/h is depicted in 2.2. It rises nearly linearly with increasing power demand. Due to the decreasing electrical efficiency of PEMFCs (see Fig. 5 in this section) at higher loads, more hydrogen is needed to reach the power setpoint. No significant differences can be observed for the different return temperatures (40, 50, and, 60 °C).

In order to assess the usability in residential applications, the flow temperature is an important characteristic as it represents the highest temperature that can be extracted to a heating circuit. The flow temperature of the FC coolant circuit depicted in 3.1 generally rises with higher power setpoints from 20 kW onwards. For 40 °C and 50 °C return temperature, the flow temperature declines between 10 kW and 20 kW. Furthermore, at these temperatures very similar flow temperatures are observed, while for the operation at 60 °C higher flow temperatures are measured. In order to achieve optimal membrane humidity, and thus optimal efficiency, the stack temperature is actively controlled by an electric temperature control valve and a humidifier based on a model-based estimation of the water in the ambient air [14]. By controlling the stack temperature, the flow temperature is directly influenced as a result. Consequently, at 40 °C and 50 °C the operation is controlled by the module towards the same thermal operating point, resulting in similar characteristics for the two return temperatures. At 60 °C return temperature, a different thermal operating point is reached resulting in higher flow temperatures. In general flow temperatures of 60 °C and above are well suited to meet residential heating and hot water demands. The same operation pattern between the different return temperatures can be observed for the flue temperature in 3.2. Again at 40 °C and 50 °C controlling towards the same thermal operating point results in very similar temperatures, while at 60 °C a different operating point is reached due to the high return temperature. At these return temperatures, the heat cannot be dissipated with the same efficiency resulting in more waste heat being ejected.

Fig. 4 shows the combined extracted thermal power of the BOP and FC circuit at different electrical power setpoints and return temperatures. For lower return temperatures more thermal power is extracted at the heat exchangers, as the heat can be dissipated with higher efficiency compared to the operating point at higher return temperatures of 60 °C. As the electrical efficiency falls at higher loads and the thermal efficiency rises (see Fig. 5 in the next part of this section), the thermal power does not rise linearly, but exhibits a steeper slope at higher power setpoints, similar to the hydrogen consumption of the module seen in 2.2.

Fig. 5 shows the electrical, thermal and total efficiency with respect to the HHV as a function of the power setpoint. It should be noted, that the potential energy within the hydrogen due to the compression would reduce the stated efficiencies by about 1.95%, however this reduction is not included in the figure. This approach was chosen to maintain comparability with other CHP systems and fuel cells, for

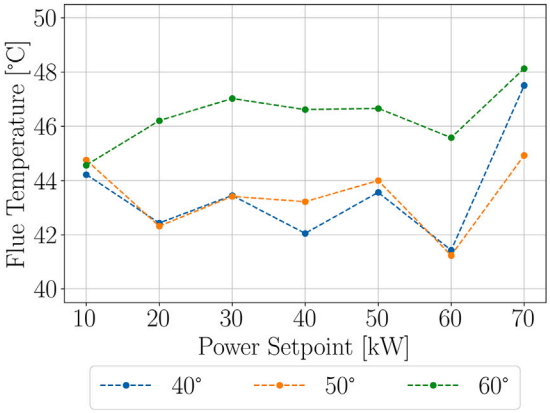


Fig. 3.2. Flue Temperature. Similar to the flow temperatures, the flue temperature (T_{Flue}, see Fig. 1) at 40 °C and 50 °C return temperature is very similar while it becomes higher for 60 °C return temperature.

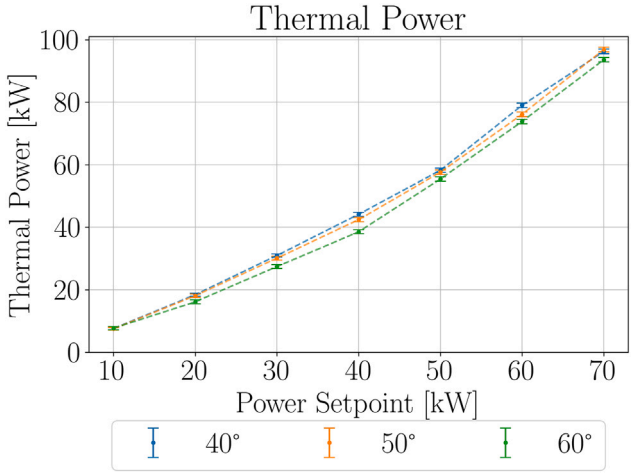


Fig. 4. Thermal Power. Comprehensively the thermal power extracted rises with the electrical power. Again for 40 °C and 50 °C return temperatures the thermal power is very similar, while it becomes smaller at 60 °C return temperature.

which it is common practice to define the system boundaries such that the pressure-related potential energy of the supplied fuel is excluded.

In our tests we reached a maximum total efficiency of 97.1% at 40 kW and 40 °C FC return temperature. At 40 °C and 50 °C the module operates at very similar efficiencies. At 60 °C more heat is lost through the exhaust gas 2.1, as the heat is dissipated with less efficiency in the cooling circuit at this temperature. This results in significantly lower thermal efficiency. The electrical efficiency is not affected by the FC return temperature and declines at higher power setpoints. This general behavior is expected for PEMFCs. In order to achieve a higher power output, the current of the FC stack increases, which causes the voltage to decline due to higher activation, ohmic and mass-transport losses. As these losses ultimately result in more waste heat, more heat can be dissipated by the cooling circuits causing an increase in thermal power (see Fig. 4) [34]. This shift results in relatively constant total efficiencies between 20 kW and 60 kW for 40 °C and 50 °C. These very high efficiencies align with computed values of simulation studies investigating the potential of PEMFC systems in CHP configuration [28,32]. Existing experimental studies offer limited comparability, due to different system borders [17,24,26], different heat recovery methods [25] or different power classes [27]. Nonetheless, the highest found experimentally measured efficiencies of a PEMFC in CHP configuration are 93% [17] and 92% [24].

In a modern low-energy building household, equipped with an EV charging station, electricity accounts for approximately 42% of the total energy demand, while space heating represents the remaining 58% [35,36]. In particular, the high electrical efficiencies compared to classical CHP systems [37–39] offer significant advantages when combined with a heat pump: during winter, when heat demand dominates, a heat pump effectively amplifies the useful thermal energy delivered from the generated electricity. Conversely, during summer, when heat demand is low or absent, higher electrical efficiencies reduce the required fuel consumption.

4. Summary and conclusions

In this work, we present for the first time the results of operating a mobile Honda fuel cell module on a stationary test bench in CHP configuration. During our tests on the test bench, we have analyzed multiple characteristics for three different FC return temperatures (40, 50, and, 60 °C). Among these characteristics is the hydrogen concentration in the exhaust gas during steady state operation. Our results show that nearly no hydrogen is lost via the exhaust gas, marking an improvement regarding exhaust purity when compared with previous studies [17,23]. Furthermore, it was observed that the very low hydrogen concentration in the exhaust gas occurs normally only during start-up and shut-down procedures of the system. From a technical point of view, setups might be possible to capture the exhaust gas during these procedures instead of releasing it directly into the atmosphere. With this consideration, no hydrogen would be released, which would avoid the secondary greenhouse gas effect associated with hydrogen emissions. The fact of the almost negligible hydrogen in the exhaust contributes to the high efficiencies of up to 97.1%. In addition to the hydrogen concentration in the exhaust gas, we measured the hydrogen flow at the inlet during operation, which does not vary significantly for the different return temperatures.

The flow temperature offers insights into possible real world CHP applications of this FC module in residential areas. With a flow temperature of 60 °C and higher, this module is well suited to generate heat for residential heating circuits, which require a temperature above 60 °C. Additionally, higher return temperatures result in higher flow temperatures facilitating utility in a wide range of residential applications.

The most important result is likely represented by the efficiency. Although this module was initially optimized for mobile applications, very high thermal and electrical efficiencies of over 54% and 50% respectively and a total efficiency of up to 97.1% (HHV) have been achieved in stationary application. The energy production at the optimal operating point according to our measurements at 40 kW electrical power setpoint and 40 °C return temperature, amounts to 39.8 kWh/kg_{H_2}. These results highlight the potential of this system to serve as a highly efficient stationary power and heat source for residential applications and critical infrastructure, such as hospitals, and represent a significant improvement over commercially available hydrogen combustion engine CHP systems [40,41]. Other experimental studies often come with a different scope, limiting the comparability (see Table 1). Nonetheless, the efficiency measurements of the studied module significantly exceed previously studied PEMFC-based CHP systems, which reached efficiencies of up to 93% [6,8] (see also Table 1). These results strongly support the use of serially produced FC modules for mobile applications as flexible, decentralized and highly efficient stationary combined heat and power generation units, which have the potential of increasing the energy system's independence and resilience.

The focus of the study is the system level investigation of serially produced FC modules, that leverage economies of scale. Thus, the interpretations and analyses of the results are limited to the system level and do not include stack level investigations. Furthermore, only steady state operation is examined. Characteristics of highly dynamic operations have not been studied. The components such as the stack,

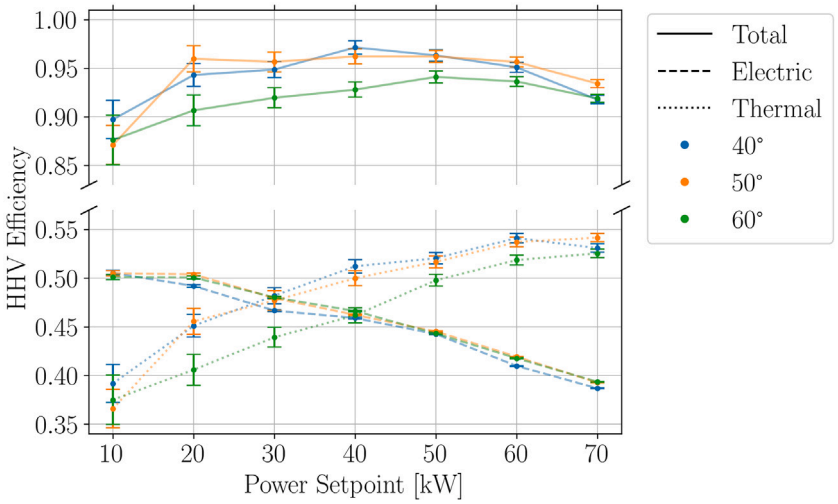


Fig. 5. Efficiencies of the FC Module. The electrical efficiency falls with rising power setpoint while the thermal efficiency increases. In general at 60 °C FC return temperature the efficiency is lower compared to 40 °C and 50 °C. The efficiency is calculated with respect to the HHV.

the air compressor, the cooling circuits and the control mechanisms of the investigated FC system are already completely designed and thoroughly tested and optimized. Directly transferring such a FC system into stationary application has practical advantages as the design and optimization process of the stack and the various subsystems have already been done. Consequently, the focus can lie on technical challenges such as the design of the heat recovery, the efficient utilization of the module, the efficient design and sizing of necessary connections and of auxiliary and safety systems and its embedding into an existing energy system as a resilient, decentral and flexible energy source. This approach can offer synergies between different sectors of the economy leading to reduced capital costs and thus more widespread adoption. The investigated power class is well suited to supply decentral residential quarters, aiding the transition to a renewable and resilient energy system.

5. Outlook

With the provided test procedure, the description of the test bench setup and the sensor list, the results should be reproducible. Particular attention should be paid to the insulation of the module and especially the pipes, as the losses in the cooling circuits and consequently in the thermal efficiency depend on the insulation.

The results show that the analyzed FC module operates highly efficient in stationary CHP configuration and holds great promise for decentralized applications. Based on the energy demand profiles of modern low-energy buildings equipped with EV charging infrastructure, a single fuel cell of the type investigated in this study could supply approximately ten single-family households [35,36]. This number could be increased substantially through the integration of complementary technologies such as heat pumps, electrical battery storage, and thermal energy storage systems. To further underline its usage in such a context, more research will be conducted in the future. This future research comprises multiple use-cases, including the application as a thermal and electrical power source in residential areas as well as an auxiliary power source for electric vehicle charging stations. These application cases will be outlined in more detail and simulated using the characteristics from the present study.

CRediT authorship contribution statement

Antonius Tilgner: Writing – review & editing, Writing – original draft, Visualization, Validation, Software, Methodology, Investigation, Formal analysis, Data curation, Conceptualization. **Johannes Seesing:** Writing – review & editing, Writing – original draft, Validation, Software, Project administration, Methodology, Investigation, Formal analysis, Data curation, Conceptualization. **Heinz Bekebrok:** Writing – review & editing, Validation, Supervision, Methodology, Investigation, Conceptualization. **Marco Ohm:** Supervision, Methodology, Conceptualization. **Alexander Dyck:** Writing – review & editing, Project administration, Funding acquisition. **Sebastian Barth:** Writing – review & editing, Project administration, Conceptualization. **Florian Rass:** Conceptualization. **Yannick Arz:** Validation, Data curation, Conceptualization. **Thomas Brachmann:** Conceptualization. **Hendrik Langnickel:** Writing – review & editing, Supervision, Project administration, Methodology, Investigation, Funding acquisition, Conceptualization.

Declaration of AI and AI-assisted technologies in the writing process

During the preparation of this work, the authors utilized OpenAI's *ChatGPT*, Meta's *LLaMA* on an internal system and *DeepL* as programming assistants and in order to improve the style of writing. After using these tools/services, the authors reviewed and edited the content as needed and take full responsibility for the content of the publication.

Declaration of competing interest

The authors declare that they have no known competing financial interests or personal relationships that could have appeared to influence the work reported in this paper.

Acknowledgments

We would like to acknowledge the contribution of Jens Fröhlich and Jonas Hilling of H2 Powercell GmbH to the programming of the communication between the module and the test rig. We also thank Lars Höpken for his extensive support during the set up and the programming of the test bench in time-critical phases of the project.

Table A.2
Overview of relevant sensors together with their respective systematic errors as depicted in the schematic flowchart (Fig. 1).

Name	Description	Type of sensor	System error
$T_{FC,hot}$	Temperature sensor	PT100 DIN EN 60751, Kl. A	±0.15 °C
$T_{FC,cold}$	Temperature sensor	PT100 DIN EN 60751, Kl. A	±0.15 °C
$T_{BOP,hot}$	Temperature sensor	PT100 DIN EN 60751, Kl. A	±0.15 °C
$T_{BOP,cold}$	Temperature sensor	PT100 DIN EN 60751, Kl. A	±0.15 °C
T_{Flue}	Temperature sensor	PT100 DIN EN 60751, Kl. A	±0.15 °C
T_{Flow}	Temperature sensor	PT100 DIN EN 60751, Kl. A	±0.15 °C
F_{FC}	Magnetic-inductive flow sensor	IFM_SM7020	±0.8%
F_{BOP}	Magnetic-inductive flow sensor	IFM_SM6020	±0.8%
F_{H_2}	Thermal mass flow sensor	Bronkhorst EL-FLOW Select F-113AC-1M0	±0.5%
C_{H_2}	Thermal mass flow sensor	Neoxid NEO974HT	±0.3 $vol.\%_{H_2}$

Additionally, the authors thank the Federal Ministry for Economic Affairs and Energy for financial support within the project HyNRGCube (reference number 03EN5045D) on the basis of a decision by the German Bundestag.

Appendix. List of sensors

See Table A.2.

Data availability

The data that has been used is confidential.

References

[1] G.S. Seck, E. Hache, J. Sabathier, F. Guedes, G.A. Reigstad, J. Straus, O. Wolfgang, J.A. Ouassou, M. Askeland, I. Hjorth, H.I. Skjelbred, L.E. Andersson, S. Douguet, M. Villavicencio, J. Trüby, J. Brauer, C. Cabot, Hydrogen and the decarbonization of the energy system in europe in 2050: A detailed model-based analysis, Renew. Sustain. Energy Rev. 167 (2022) 112779, http://dx.doi.org/10.1016/j.rser.2022.112779.

[2] S. Shahzad, T.R. Alsenani, O. Alrumayh, A. Altamimi, H. Kilic, Adaptive hydrogen buffering for enhanced flexibility in constrained transmission grids with integrated renewable energy system, Int. J. Hydrog. Energy 144 (2025) 637–651, http://dx.doi.org/10.1016/j.ijhydene.2025.02.316.

[3] A. Orths, C.L. Anderson, T. Brown, J. Mulhern, D. Pudjianto, B. Ernst, M. O'Malley, J. McCalley, G. Strbac, Flexibility from energy systems integration: Supporting synergies among sectors, IEEE Power Energy Mag. 17 (2019) 67–78, http://dx.doi.org/10.1109/MPE.2019.2931054.

[4] B. Urishev, Decentralized energy systems, based on renewable energy sources, Appl. Sol. Energy 55 (2019) 207–212, http://dx.doi.org/10.3103/S0003701X19030101.

[5] S. Yu, Y. Fan, Z. Shi, J. Li, X. Zhao, T. Zhang, Z. Chang, Hydrogen-based combined heat and power systems: A review of technologies and challenges, Int. J. Hydrog. Energy (2023) http://dx.doi.org/10.1016/j.ijhydene.2023.05.187.

[6] V. Cigolotti, M. Genovese, P. Fragiacomo, Comprehensive review on fuel cell technology for stationary applications as sustainable and efficient poly-generation energy systems, Energies 14 (16) (2021) 4963, http://dx.doi.org/10.3390/en14164963.

[7] E.R. Nielsen, C.B. Prag, T.M. Bachmann, F. Carnicelli, E. Boyd, I. Walker, L. Ruf, A. Stephens, Status on demonstration of fuel cell based micro-CHP units in europe, Fuel Cells 19 (4) (2019) 340–345, http://dx.doi.org/10.1002/fuce.201800189.

[8] W. Gao, P. Dong, Y. Hu, Y. Wang, H. Yang, L. Yang, M. Yang, Progress on residential fuel cell combined heat and power systems: A technological review, Renew. Sustain. Energy Rev. 226 (2026) 116273, http://dx.doi.org/10.1016/j.rser.2025.116273.

[9] Y. Budak, Y. Devrim, Investigation of micro-combined heat and power application of PEM fuel cell systems, Energy Convers. Manage. 160 (2018) 486–494, http://dx.doi.org/10.1016/j.enconman.2018.01.077.

[10] W.-J. Zou, K.-Y. Shen, S. Jung, Y.-B. Kim, Application of thermoelectric devices in performance optimization of a domestic PEMFC-based CHP system, Energy 229 (2021) 120698, http://dx.doi.org/10.1016/j.energy.2021.120698.

[11] N. Briguglio, M. Ferraro, G. Brunaccini, V. Antonucci, Evaluation of a low temperature fuel cell system for residential CHP, Hysydays, Int. J. Hydrog. Energy 36 (13) (2011) 8023–8029, http://dx.doi.org/10.1016/j.ijhydene.2011.01.050.

[12] P. Xie, F. Zhou, S. Tan, V. Liso, S.L. Sahlin, Development of a two-layer control and management system for a residential microgrid with HT-PEMFC-based micro-CHP, Appl. Energy 381 (2025) 125118, http://dx.doi.org/10.1016/j.apenergy.2024.125118.

[13] A. Kampker, H. Heimes, M. Kehrer, S. Hagedorn, P. Reims, O. Kaul, Fuel cell system production cost modeling and analysis, Energy Rep. 9 (2023) 248–255, http://dx.doi.org/10.1016/j.egyr.2022.10.364.

[14] Honda Motor Co., Ltd., Hydrogen fuel cell system, 2024, https://global.honda/en/tech/Hydrogen_Fuel_Cell_System_FC/. (Accessed 12 March 2026).

[15] T. Tiedemann, M. Kroener, M. Vehse, C. Agert, Fuel cell electrical vehicles as mobile coupled heat and power backup-plant in neighbourhoods with low-energy standards buildings, in: 6th E-Mobility Power System Integration Symposium (EMOB 2022), vol. 2022, 2022, pp. 122–128, http://dx.doi.org/10.1049/icp.2022.2725.

[16] T. Tiedemann, M. Kroener, M. Vehse, C. Agert, Fuel cell electrical vehicles as mobile coupled heat - and power plant for domestic use during "dunkelflauten", in: 2021 Sixteenth International Conference on Ecological Vehicles and Renewable Energies, EVER, 2021, pp. 1–8, http://dx.doi.org/10.1109/EVER52347.2021.9456614.

[17] B.M. Alves, P. Savignac, P. Leduc, Energy balance and hydrogen exhaust emissions of the second-generation toyota mirai, Int. J. Hydrog. Energy 156 (2025) 150411, http://dx.doi.org/10.1016/j.ijhydene.2025.150411, URL https://www.sciencedirect.com/science/article/pii/S0360319925034093.

[18] H. Lohse-Busch, K. Stutenberg, M. Duoba, X. Liu, A. Elgowainy, M. Wang, T. Wallner, B. Richard, M. Christenson, Automotive fuel cell stack and system efficiency and fuel consumption based on vehicle testing on a chassis dynamometer at minus 18°c to positive 35°c temperatures, Int. J. Hydrog. Energy 45 (1) (2020) 861–872, http://dx.doi.org/10.1016/j.ijhydene.2019.10.150, URL https://www.sciencedirect.com/science/article/pii/S0360319919339618.

[19] J. Sery, P. Leduc, Fuel cell behavior and energy balance on board a hyundai nexo, Int. J. Engine Res. 23 (5) (2022) 709–720, http://dx.doi.org/10.1177/14680874211059046, arXiv:https://doi.org/10.1177/14680874211059046.

[20] G. Di Pierro, E. Bitsanis, A. Tansini, C. Bonato, G. Martini, G. Fontaras, Fuel cell electric vehicle characterisation under laboratory and in-use operation, Energy Rep. 11 (2024) 611–623, http://dx.doi.org/10.1016/j.egyr.2023.12.013, URL https://www.sciencedirect.com/science/article/pii/S2352484723016050.

[21] K. Jennifer, S. Sam, A. Chris, S. Genevieve, J. Matt, Fuel cell electric vehicle evaluation, 2016, https://www.hydrogen.energy.gov/docs/hydrogenprogramlibraries/pdfs/review16/tv001_kurtz_2016_o.pdf. (Accessed 14 March 2026).

[22] E. Chojkiewicz, A. Phadke, Leveraging automotive fuel cells can supply zero-emission peak power in the near-term, IScience 27 (7) (2024) 110246, http://dx.doi.org/10.1016/j.isci.2024.110246.

[23] D. Pearman, W. Buttner, A. Loiselle-Lapointe, A. Conde, Fuel cell vehicle hydrogen emissions testing, in: 2023 International Conference on Hydrogen Safety, 2023.

[24] Z. Hua, J. Wu, J. Tang, X. Cao, S. Cai, Z. Tu, Multi-stack pemfc cogeneration system with integrated multi-recovery: experimental characterization and optimization, Applied Energy 420 (2026) 128194, http://dx.doi.org/10.1016/j.apenergy.2026.128194.

[25] X. Lu, B. Du, W. Zhu, Y. Yang, C. Xie, Z. Tu, B. Zhao, L. Zhang, J. Song, Z. Deng, Thermodynamic and dynamic analysis of a hybrid pemfc-orc combined heat and power (chp) system, Energy Conversion and Management 292 (2023) 117408, http://dx.doi.org/10.1016/j.enconman.2023.117408.

[26] G. Singer, P. Pertl, A. Trattner, Experiments on maximizing hydrogen utilization and efficiency in a pem fuel cell system, International Journal of Hydrogen Energy 106 (2025) 1158–1166, http://dx.doi.org/10.1016/j.ijhydene.2025.02.036.

[27] C. Davila, N. Paulus, V. Lemort, Experimental investigation of a micro-chp unit driven by natural gas for residential buildings, 2022.

[28] A. Herrmann, A. Mädlow, H. Krause, Key performance indicators evaluation of a domestic hydrogen fuel cell chp, A Special Issue with the Papers Selected from the 7th World Hydrogen Technologies Convention, International Journal

of Hydrogen Energy 44 (35) (2019) 19061–19066, http://dx.doi.org/10.1016/j.ijhydene.2018.06.014.

[29] H. Chang, X. Xu, J. Shen, S. Shu, Z. Tu, Performance analysis of a micro-combined heating and power system with pem fuel cell as a prime mover for a typical household in north china, International Journal of Hydrogen Energy 44 (45) (2019) 24965–24976, http://dx.doi.org/10.1016/j.ijhydene.2019.07.183.

[30] Y. Wang, Z. Zeng, T. Wang, Z. Che, Dynamic simulation and optimization of a residential proton exchange membrane fuel cell (pemfc) combined heat and power (chp) system, Energy 319 (2025) 134865, http://dx.doi.org/10.1016/j.energy.2025.134865.

[31] M. Gandiglio, A. Lanzini, M. Santarelli, P. Leone, Design and optimization of a proton exchange membrane fuel cell chp system for residential use, Energy and Buildings 69 (2014) 381–393, http://dx.doi.org/10.1016/j.enbuild.2013.11.022.

[32] X. Lyu, Y. Yuan, W. Ning, L. Chen, W.-Q. Tao, Investigation and optimization of pemfc-chp systems based on chinese residential thermal and electrical consumption data, Applied Energy 356 (2024) 122337, http://dx.doi.org/10.1016/j.apenergy.2023.122337.

[33] E.O. Lebigot, Uncertainties: a python package for calculations with uncertainties, Tech. Rep. / Softw. Doc. (2010) URL https://pythonhosted.org/uncertainties/.

[34] Eg&g Technical Services and of Energy Inc., U. S. Department, Fuel Cell Handbook (Seventh Edition), Lulu.com, 2016.

[35] M. Schlemminger, T. Ohrdes, E. Schneider, M. Knoop, Dataset on electrical single-family house and heat pump load profiles in germany, Scientific Data 9 (1) (2022) 56, http://dx.doi.org/10.1038/s41597-022-01156-1.

[36] E. Sperber, C. Schimeczek, U. Frey, K.K. Cao, V. Bertsch, Aligning heat pump operation with market signals: a win-win scenario for the electricity market and its actors?, Energy Reports 13 (2025) 491–513, http://dx.doi.org/10.1016/j.egyr.2024.12.028.

[37] M. Badami, A. Casetti, P. Campanile, F. Anzioso, Performance of an innovative 120 kwe natural gas cogeneration system, Energy 32 (5) (2007) 823–833, http://dx.doi.org/10.1016/j.energy.2006.06.006.

[38] X.L. Zhao, L. Fu, S.G. Zhang, Y. Jiang, H. Li, Performance improvement of a 70 kwe natural gas combined heat and power (chp) system, Demand Response Resources: The US and International Experience, Energy 35 (4) (2010) 1848–1853, http://dx.doi.org/10.1016/j.energy.2010.01.005.

[39] D. Wijesekara, P. Amarasinghe, A. Induranga, V. Vithanage, K.R. Koswattage, Energy, exergy, and environmental impact analysis and optimization of coal–biomass combustion combined cycle chp systems, Sustainability 17 (6) (2025) 2363, http://dx.doi.org/10.3390/su17062363.

[40] G.E. A.G., Effizienz in reinkultur, 2025, URL https://2-g.com/de/produkte/kwk-anlagen/agenitor.

[41] Bosch Thermotechnik GmbH, BHKW TEDOM von 30 bis 530 kw, 2025, URL https://www.buderus.de/de/produkte/bhkw-tedom-von-30-bis-530-kw–73546.